(De-)Multiplexing: Multi-Trap Force Measurements and Sample Manipulation with JPK's NanoTracker™ 2

Optical tweezers utilize the fundamental property of light to carry linear and angular momentum in order to trap objects with a highly focused laser beam. This technique allows the direct manipulation of microscopic objects with sizes from few tens of nanometers up to several micrometers. Furthermore, optical tweezers are a quantitative tool to apply well-defined forces and, at the same time, accurately measure displacements of and forces acting on the trapped object. This combination of non-invasive microscopic manipulation and simultaneous high precision measurements has made optical tweezers a useful and versatile tool in a variety of applications ranging from micro-rheology and colloidal hydrodynamics to molecular biochemistry, biophysics and cell biology.

While many measurements (e.g. hydrodynamics, micro-rheology, tracking of protein motion) can be performed with single traps in combination with a piezo-electric high-precision sample scanner, other applications like whole cell rheology and the manipulation of complex multi-molecular systems often require multiple traps that can be positioned individually. Example experimental setups are shown in figure 1. In many cases, the requirements even go beyond mere trap positioning and include the parallel measurement of forces acting on multiple trapped particles. More details on diverse optical trapping applications and techniques can be found in the comprehensive review by Moffit *et al*. [1].

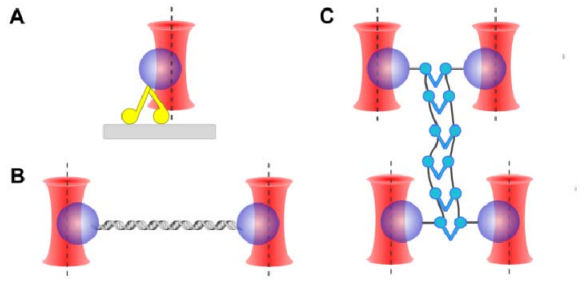

Figure 1 *Different applications require single- double- or multi-trap configurations.* ***A*** *The tracking of motor proteins or other objects in x/y can be performed with a single trap and piezo scanners.* ***B*** *Stretching macromolecules like DNA or whole cells in solution requires at least two independent traps.* ***C*** *Complex arrangements of multiple molecules e.g. to measure DNA-protein interactions can only be implemented with a multitude of independently controlled traps.*

Double trap configurations

Dual beam traps are typically generated by polarization-dependent beam splitting of a single laser source [2]. Here the incoming light is linearly polarized and subsequently split in two beams with perpendicular orientation. This minimizes interference between the two traps in the sample and enables the separate detection of signals from the traps. In JPK's NanoTracker™ 2, at least one of these traps can be positioned individually via piezo-electric mirrors or acousto-optical deflectors (AODs). This provides the necessary degrees of freedom for a wide range of measurements like single molecule stretching or basic whole cell manipulation. Due to the polarization-based separation of the two beams, the highest possible measurement accuracy is also ensured for dual-trap setups.

Multiplexing

For many applications, it is favorable or even necessary to manipulate a sample optically at many locations at the same time. Prominent examples would be the handling of multi-molecular constructs with several attached micro-bead handles (see figure 1), the manipulation of suspended cells and particles in order to investigate their interactions, or the deformation of cells and other objects in complex patterns.

For these purposes, multiple (more than two) independent traps can be set up from one single laser source. This method termed *multiplexing* can be implemented by moving the beam quickly from one desired trap position to the next where it resides for a defined time (*dwell time*, t_{dw}) and thus establishes the conditions for optical trapping [3]. The time course of this beam position switching is illustrated in figure 2. This approach to multiplexing is called *time-sharing* (or *beam-*

sharing) and, depending on the laser power, enables the creation of tens to hundreds of parallel traps at independent positions in the sample. The method is technically very demanding and requires precise and fast control electronics as well as high speed beam positioning. For stable trapping, the dwell time has to be longer than the time scale of the particle's Brownian motion under the given conditions. For Polystyrene (PS) beads in the size range of $1-2\,\mu m$ in water, the lower limit for t_{dw} is typically between 20 and $50\,\mu s$.

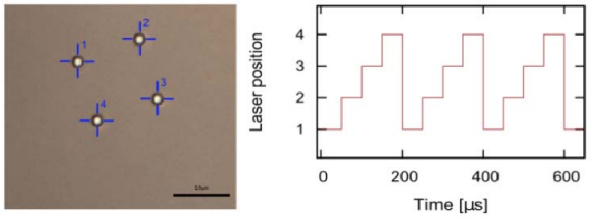

Figure 2 *Time sharing priciple. Four traps are set up by fast switching of the laser position. Left: bright field image of four polystyrene beads (PS, $d = 1.53\,\mu m$) caught in parallel traps. Right: Illustration of the laser movement. The laser resides at each trap position for a defined time t_{dw} (here: $50\mu s$) before it moves to the next location. With this method, multiple stable traps can be generated*

The second limiting time factor is the so called *revisiting time* t_{rev} , that is the time that passes until the laser beam has cycled through all trap positions and returns to the same spot (i.e. the time a trapped particle is without laser). Uninterrupted manipulation requires that the object cannot escape the trap volume while the laser is scanning the other trap positions. Just like t_{dw}, t_{rev} depends on particle size as well as medium temperature and viscosity and needs to be determined for each experimental setup. Typical values are in the range of a few milliseconds.

Naturally, the achievable revisiting times also depend on the number of traps N to be implemented:

$$t_{rev} = (N-1)\,t_{dw}$$

Large numbers of parallel traps with revisiting times shorter than $10\,ms$ in turn require very high switching rates f_s of the beam positioning devices:

$$f_{switch} = N/t_{rev}$$

For $t_{rev} \leq 10ms$ and $N = 250$ parallel traps, this yields

$$f_{switch} \geq \frac{250}{10ms} = 25kHz$$

In JPK's NanoTracker™ 2, an ultra-fast AOD ensures that the above conditions for stable trapping and manipulation are maintained even for hundreds of simultaneous traps. An example of trap multiplexing with 80 parallel traps is shown in figure 3

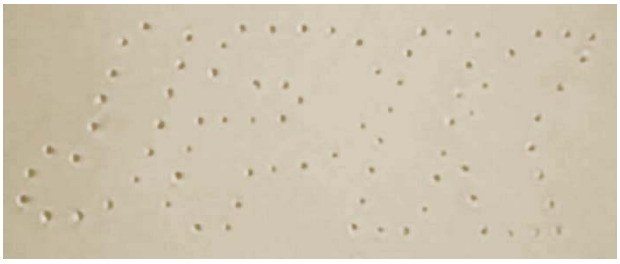

Figure 3 *1µm silica beads in multiplexed traps. 80 particles are trapped simultaneously and arranged to form the JPK company logo. Ultrafast AODs allow the parallel trapping and manipulation of hundreds of particles.*

Trap stiffness

The stiffness of an optical trap denotes the restoring forces acting on a trapped particle per displacement from the trap center and depends on numerous parameters. Among them, the most important are laser power and beam shape, the size of the trapped object, the ratio of refractive indices ($n_{particle}/n_{medium}$), and the steepness of the intensity gradient in the focal spot. In multiplexed traps, the gradient force $\boldsymbol{F_G}$ responsible for centering the trapped particle in the focused laser beam is only acting on each object during the dwell time t_{dw} (i.e. while the laser is present at the respective position) and is absent for t_{rev}. Thus, the trap stiffness is also "shared" among multiplexed traps. For scanning frequencies above the corner frequency of the particle's Brownian motion power spectrum ($\approx 250-1500\,Hz$ for micrometer-sized particles, see figure 7 and JPK's technical note on quantitative force measurements with optical tweezers), the effective trap stiffness decreases linearly with the number of parallel traps [4]. By varying t_{dw} for different positions, traps with different stiffness values can be

generated from one single laser beam. This function is conveniently integrated in the NanoTracker™ 2 control software where the position and dwell time for each of the multiplexed traps can be set separately or optionally all traps can be synchronized to have the same effective trap stiffness (see figure 4). A widely used application of optical tweezers is the manipulation and deformation of live suspended cells (e.g. red blood cells) for rheological measurements. With the different force levels available for multiplexed traps in the NanoTracker™ 2, cells can be held and positioned with minimum forces in order not to disturb the deformation-force measurements that are conducted simultaneously with two stronger traps. Moreover, multi-molecular arrangements, macro-molecules or nano-fabricated devices can be stably held at constant positions with multiple stronger traps while a weaker trap is used to probe their properties or interactions with other objects.

Force measurements with multiplexed traps: de-multiplexing

Since multiplexed traps are all derived from the same beam, they do not differ in polarization and cannot be separated easily for individual analysis like the two beams used for dual trap configurations. This means that the signals from all multiplexed traps are recorded with one quadrant photo diode (QPD). This renders the standard noise spectrum based calibration method (and thus the determination of detection sensitivity and trap stiffness) unfeasible without further data processing. The challenge is to separate the signals originating from different trap positions in order to make sure that only Brownian motion data of the same trap and particle are

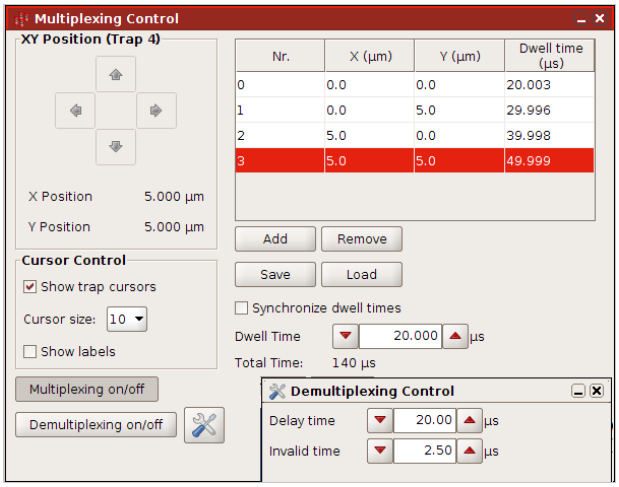

Figure 4 *NanoTracker™2 software control panel for convenient configuration of multiple parallel traps in the time-sharing mode. In addition to mouse control, traps can be precisely set by numerical coordinates. Individual dwell times for different trap stiffnesses (see main text) allow a multitude of trap variations.. Saving and loading of configuration files facilitates the handling of complex multi-trap setups. Parameters for precise force and position measurements in up to eight parallel traps can be set in the de-multiplexing control panel (de-multiplexing mode, discussed below).*

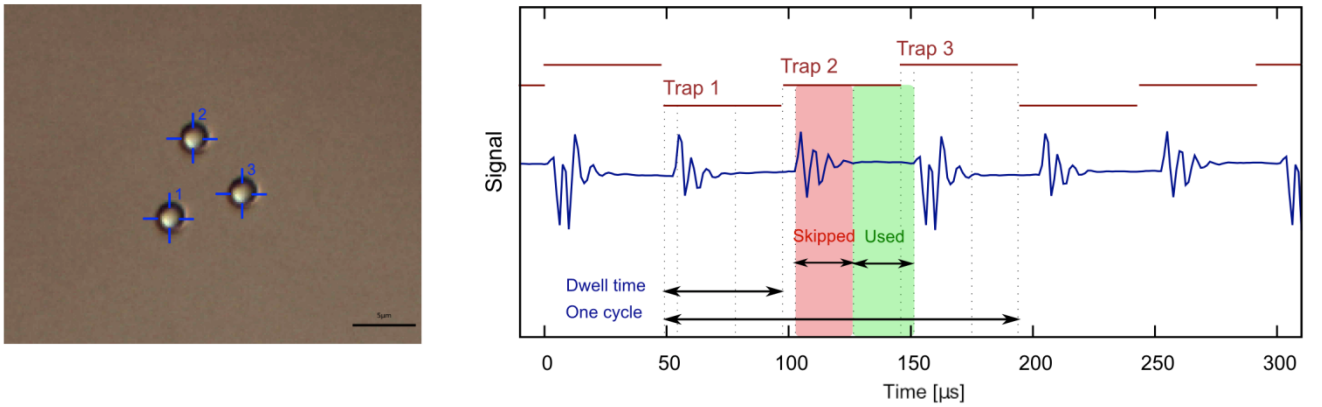

Figure 5 *Three parallel traps set up in the time-sharing mode.* ***Left****: Bright field image of PS-beads in parallel traps.* ***Right****: raw signal from the QPD containing the signals from all three traps. Red lines indicate the electronically triggered dwell times for positioning the laser beam at the respective traps. The phase marked in red (invalid time) is the time the AOD needs to reposition the laser beam. It is not used for further data processing and trap signal separation. The small offset between the beginning of the dwell time and the repositioning of the laser results from system internalt data transfer. For optimal signal separation, both values (delay time and invalid time) can be set in the de-multiplexing control panel (see Figure 4).*

used for calibration of the individual traps. The graph in figure 5 shows the raw signal of three multiplexed traps as it is recorded by the QPD. The NanoTracker™ 2 detection system and data processing electronics operate at a frequency of $800\ kHz$ which allows to time-resolve the different phases of trap multiplexing following the approach introduced by Guilford *et al*. [5]. It is clearly visible that the traps produce slightly different plateaus of thermal noise signals which are interrupted by higher amplitude signals caused by the position switching process. These plateau phases as well as the characteristic shape of the switching transition help to identify the times when the laser beam is present and stable at the positions of trap 1 to 3. Time delays inherent to the system can be estimated and taken into account. In the de-multiplexing control panel shown in figure 4, values for the *delay time* t_{lag} and the time required for position switching (*invalid time*) can be set matching the current trap configuration. After identifying t_{lag} as well as the switching and effective dwelling phases, the signal from one dwelling phase is averaged for further data processing. These average values (one per trap and cycle) are then used to generate the separated signals from the multiplexed traps. A typical example of such an extracted signal for one trap is shown in figure 6. On longer time scales (left graph), the signals appear like

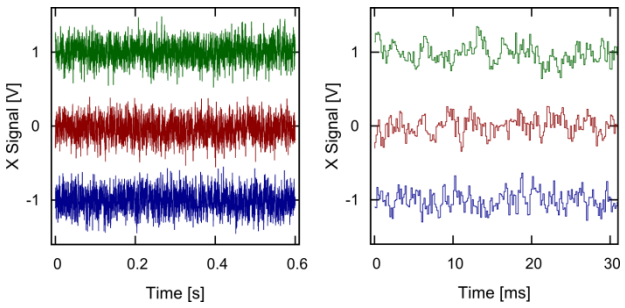

Figure 6 *With delay and invalid times set to the correct values for the current trap configuration, the signals of multiple traps can be well isolated and evaluated separately. Left: Time-separated signals from the three multiplexed traps shown in figure 5. Right: Zooming in on the time axis reveals that the signals are reconstituted from average values and contain just one data point per cycle. For better visualization, signals from trap 2 and 3 were shifted by $\pm 1V$, respectively.*

regular constant noise as it is typically recorded from spherical particles in an optical trap. Only zooming in the time axis reveals that the signal has been reconstituted from the time separated original signal. After this averaging step, QPD signals for each of the N traps can be generated with a maximum effective sample rate of

$$f_{s,eff}^{max} = \frac{1}{t_{dw}^{min} * N} = \frac{1}{20\ \mu s * N} = \frac{50kHz}{N}$$

For the example shown in figure 4 with $N = 3$ and $t_{dw} = 50\mu s$, this means that after Fourier transforming the signal, each trap can be calibrated using a power spectrum recorded up to approximately $6.7\ kHz$ (corresponding to a time resolution of $150\ \mu s$). This in turn allows using JPK's well-established and reliable power spectrum fitting routine and to achieve the same high standard for the determination of detection sensitivity and trap stiffness in the multiplexing mode that is known from single or dual trap calibrations (figure 7). Considering the nature of this de-multiplexed signal, it is clear that frequencies higher than the effective sample rate cannot be resolved in the noise signals and are not contained in the respective power spectra.

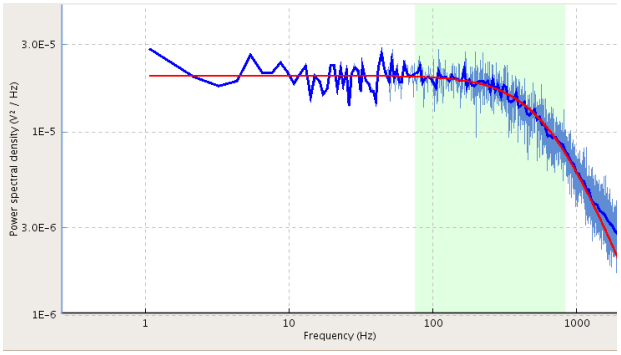

Figure 7 *Power spectrum derived from the isolated signal of one of the traps in Figure 4. After clean separation of the noise signals, power spectrum-based calibration is possible for each trap. The red line is a Lorentzian curve fitted to the data in the range highlighted in green. It is used to determine the corner frequency and to calculate detection sensitivity and trap stiffness.*

Viscous drag measurements with de-multiplexed traps

As a standard application and trap stiffness calibration method, viscous drag measurements are routinely used in various experiments. Here, the fluid-filled sample chamber is moved periodically with respect to the trapped beads, thus generating well-defined viscous drag forces acting on the particles. For low Reynolds number systems (laminar flow), the drag forces $\boldsymbol{F}_d$ on spherical objects can be calculated easily from bead radius, r, flow velocity, v, and medium viscosity, η, using Stokes' drag equation:

$$\boldsymbol{F_d} = -6\pi\eta r\, \boldsymbol{v}$$

In optical traps, this force results in a displacement of the particle from the trap center that can be measured in order to determine the trap stiffness. Vice versa, identical particles in traps with different stiffness values will show different displacements from the trap center when exposed to the same viscous drag as schematically shown in figure 8 A. As mentioned above, variations in dwell time t_{dw} of multiplexed traps result in different relative trap parameters: traps with larger t_{dw} are stiffer, following approximately a linear relation. Figure 8 B displays the displacement data from two beads trapped in multiplexed traps with $t_{dw} = 50$ (blue curve) and $100\,\mu s$ (green curve). For visualization purposes, the curves have been separated by shifting them $\pm\, 100\, nm$. It is clearly visible that the particle with $t_{dw} = 100\mu s$ shows a smaller displacement (corresponding to higher trap stiffness k) while the particle trapped with $t_{dw} = 50\,\mu s$ is displaced approximately twice as far. Using the calibration parameters obtained from individual power spectrum fits for each trap (like the one shown in figure 6) delivers the force-time curves displayed in figure 8 C. As expected after successful calibration, the drag forces measured in the three traps agree very well. Due to the linearity of Stokes' drag equation, reducing the flow speed from $200\mu m/s$ to $100\,\mu m/s$ leads to a drop in viscous drag of 50%. This is well reflected by the measured forces displayed in figure 8 D. This demonstrates that force measurements with piconewton resolution are also possible with de-multiplexed traps.

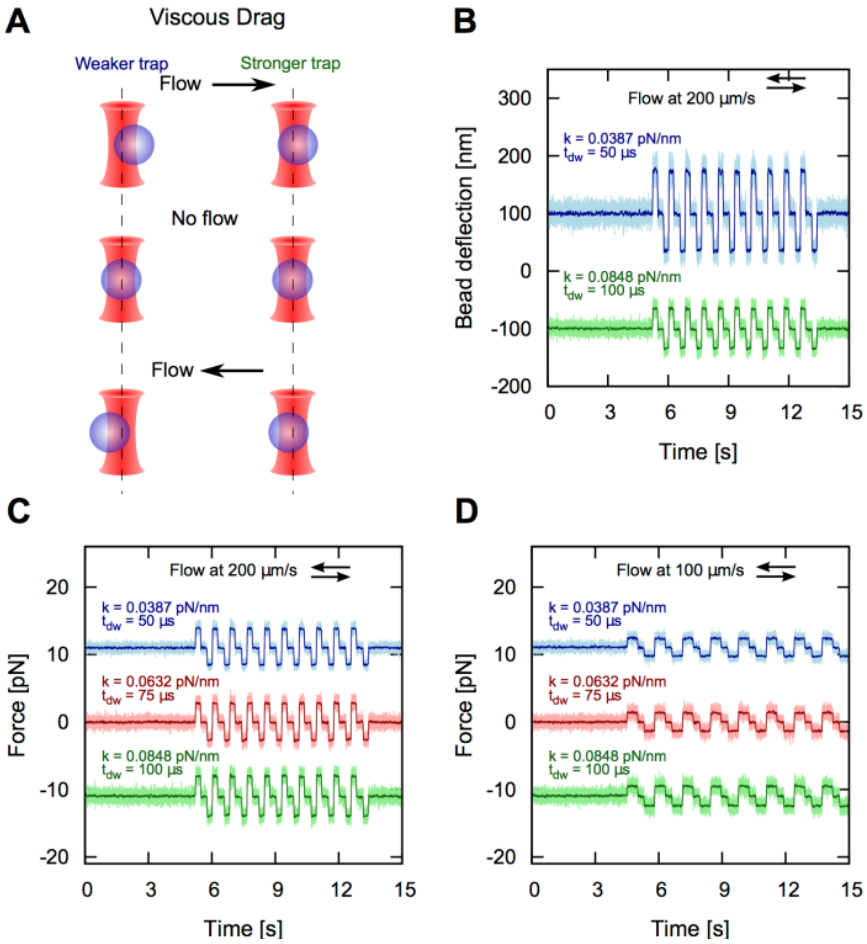

Figure 8 *Viscous drag measurements with de-multiplexed traps. A Schematic drawing of the drag force driven displacement of beads trapped with different stiffness. B Measured bead displacements under the influence of $200\,\mu m/s$ flow. The shorter dwell time $t_{dw} = 50\mu s$ results in a weaker trap and larger displacement (blue curve) while $t_{dw} = 100\,\mu s$ produces a stronger trap and smaller displacements (green curve). C After calibration of three parallel de-multiplexed traps with different dwell time (and resulting stifnesses k), the measured displacement can be converted into absolute force. The excellent agreement of all three curves indicates that in calibrated traps forces can be measured with high accuracy independent of the effective trap stiffness. D Reducing the flow speed by $\mathbf{50}\%$ results in the same reduction in drag force. Again, the amplitude of measured forces agrees very well between different traps.*

Conclusion

Trap multiplexing in the time-sharing mode of JPK's NanoTracker™ 2 relies on ultra-fast high precision beam steering and further expands the range of possible trap configurations for a multitude of applications. Trap stiffness values can be adjusted for each trap individually by the user through the convenient dwell time set function integrated in the NanoTracker™ 2 control software. All multiplexed traps can be positioned independently or arranged in complex patterns stored in custom configuration files. This freedom in configuring and dynamically rearranging tens to hundreds of parallel traps enables NanoTracker™ 2 users to perform complex manipulations of microscopic objects.

The new de-multiplexing feature is based on quick and reliable real-time data analysis and allows separating the signals from up to eight parallel traps. The isolated signals can be used for the subsequent calibration of detection sensitivity and trap stiffness which in turn is the prerequisite for high resolution displacement and force measurements. This unique combination of precision and flexibility will enable researchers to gain more detailed insight into the interactions of complex nano-scaled systems.

Literature

[1] J. R. Moffitt, Y. R. Chemla, S. B. Smith, and C. Bustamante, "Recent Advances in Optical Tweezers," *Annu. Rev. Biochem.*, vol. 77, no. 1, pp. 205–228, Jun. 2008.

[2] H. Misawa, K. Sasaki, M. Koshioka, N. Kitamura, and H. Masuhara, "Multibeam laser manipulation and fixation of microparticles," *Appl. Phys. Lett.*, vol. 60, no. 3, p. 310, 1992.

[3] K. Visscher, G. J. Brakenhoff, and J. J. Krol, "Micromanipulation by 'multiple' optical traps created by a single fast scanning trap integrated with the bilateral confocal scanning laser microscope," *Cytometry*, vol. 14, no. 2, pp. 105–114, 1993.

[4] K. Visscher, S. P. Gross, and S. M. Block, "Construction of multiple-beam optical traps with nanometer-resolution position sensing," *Ieee J. Sel. Top. Quantum Electron.*, vol. 2, no. 4, pp. 1066–1076, Dec. 1996.

[5] W. H. Guilford, J. A. Tournas, D. Dascalu, and D. S. Watson, "Creating multiple time-shared laser traps with simultaneous displacement detection using digital signal processing hardware," *Anal. Biochem.*, vol. 326, no. 2, pp. 153–166, Mar. 2004.